International Research Journal of Innovations in Engineering and Technology (IRJIET)

ISSN (online): 2581-3048

Volume 6, Issue 8, pp 61-71, August-2022

https://doi.org/10.47001/IRJIET/2022.608009

Hydrothermal Analysis of Archimedean Spiral Channel Heat Sink for CPU Cooling

[1]Hala M. Rashad, [2]Younis M. Najim, [3]Hatem Hasan Ismaeel

[1,3]Department of Energy Engineering, Technical College of Engineering, Duhok Polytechnic University, Duhok, Iraq

[2]Department of Mechanical Engineering, College of Engineering, University of Mosul- 42002, Iraq

***Abstract* - The rapid improvement of engineering modeling is supported by the improvement of parallel GPU and CPU computational capacities. However, due to space limitations, the improvement of the computational capacities of GPU and CPU imposes challenges in the cooling process. The liquid cooling method has attracted more interest as an effective heat dissipation method. In this work, a new channel configuration is introduced using the Archimedean spiral curve to generate the Archimedean spiral channel configuration. The conjugate heat sink model was created to have four different domains: liquid coolant (water), Cold plate (copper), glue layer (ethoxy), and CPU (alumina). The effect of turbulence was incorporated by varying the flow rate at a constant water inlet temperature of 25°Cto cover a range of Reynolds numbers (Re) from 3000 to 15000. The Shear Stress Transport (k-ω SST) was the used turbulent model for a better capturing of the viscous, high-frequency flow fluctuation near-wall region. Input power of 450 W was subjected to the bottom surface of the CPU. The results showed that the Reynolds number has a decisive impact on controlling the CPU temperature. As higher Re decreased the average temperature developed within the CPU and increased the pressure drop at an exponential rate. Darcy-Weisbach equation confirmed these findings for internal flow when the pressure drop depends on the squared average velocity. The hydrothermal performance of the Archimedean spiral channel configuration rapidly decreased with the Re. Similar to the velocity profile, the turbulent kinetic energy is generated at higher rate next to the channels' outer wall compared to the inner wall.**

Keywords: CPU, Liquid cooling, Heatsink, Conjugate heat transfer, Computational domain.

I. INTRODUCTION

The thermal management of electronic devices with the rapid development has become a challenging problem, where speeds of operations are really remarkable in addition to the necessity of the miniaturization of electronic devices as they have to be provided with other features like portability, adaptability and, other development needs to be used widely in industrial applications, high-performance, communication systems, computers, space shuttles, aircraft, satellites, and many other applications. The new generation of CPU and GPU are characterized by high computing power and compactness which, however, intensify the heat emission. That places the CPU and GPU at risk of malfunction or permanent damage, in order to preserve the performance of these modern high power density electronics and avoid disruption and shutting down, enhancement of cooling and thermal management becomes a necessity [1–5] therefore it's essential to use effective cooling technics as there are air cooling and liquid cooling. Air-cooled heat sinks with fans have been used conventionally for medium and low power dissipation cases[3] with increasing the heat flux, the cooling capacity could be enhanced within the system constraints by using larger heat sinks and advanced fans, however, this technique has some limitations due to air's poor heat transfer characteristics[6] therefore water-based cooling technics were utilized to avoid the disadvantages of air cooling as it has been proved that the thermal performance of liquid-based systems is significantly greater than the air-based systems due to the recent advances of nano scale and micro scale heat transfer equipment, as they might be restricted to be used for modern electronic devices [7]Different technologies of thermal management have been investigated to manage the increased heat flux[8] for instance, In 1981 Tuckerman and Pease [9] investigated the liquid-cooled micro channel heat sink with water as a coolant for removing high heat flux more than 700 W/m^2 with a pressure drop of 210 kPa and substrate temperature rise of 71 C. For better thermal management Several channel configurations were studied by researchers targeting better cooling and hydraulic performance. The channel shape effect on the heat transfer performance was investigated numerically by Khan et al. [10] as they used different shapes (straight, wavy, and dual wavy) micro-channels with different concentrations of nano-particles (1,3 and 6 %) of CuO-water at an inlet temperature of 25oC using different Reynolds number (100-900) to dissipate 200,000 W/m2 heat flux. The performance of the different micro-channels shapes was compared based on base temperature, Nusselt number, thermal performance factor, and pressure drop. It was observed that the wavy and dual-wavy channels have better performance than the straight channel. Another

International Research Journal of Innovations in Engineering and Technology (IRJIET)

ISSN (online): 2581-3048

Volume 6, Issue 8, pp 61-71, August-2022

https://doi.org/10.47001/IRJIET/2022.608009

study of swirl micro-channel heat sink cooling performance was investigated numerically by Fan et al. [11] using water as a coolant. The model consisted of several swirl channels with width and depth of 0.4 mm and 0.5 mm respectively. The channel was grooved into a circular flat plate aiming to enhance the heat transfer by generating secondary flow at higher Reynolds number. The heat sink was subjected to a heat flux of 10-60 W/cm2. The coolant entered the swirl channels at different volume flow rates ranging from 47 to 188 ml/min. It was found that the Swirl channel provided a lower temperature gradient and maximum temperature compared with the straight channel. A circular microchannel was also investigated by Jilte et al. [12] using a liquid-cooled heat sink having four channels of 3.5 mm depth and 4 mm width. The heat flux applied to the bottom surface was based on the dissipated power of 50 W and 70W. Liquid water and different types of nanofluids at different flow rates of 60 to 180 ml/min were used. Furthermore, Al-Neama et al. [13] conducted a study to examine the potential to enhance convective heat transfer and decrease the thermal resistance of a serpentine heat exchanger by adding chevron fins to it and comparing it with the conventional one, using water as a coolant at 20 °C to dissipate (100 W/cm2) using different Reynolds number of 500 to 3000. It was found that adding the chevron fins has improved the thermal performance and the Nusselt number increased by 15% while the thermal resistance and the pressure drop have decreased by 10% and 60%, respectively. In another work reported by Al-Neama[14]. He has conducted a numerical and experimental study of the thermal and hydraulic performance of three configurations; serpentine mini-channel heat sinks single, double, and triple rectangular microchannels. A comparison was made between these channel configurations with the straight microchannel in terms of Nusselt number, pressure drop, and thermal resistance. Liquid water at different flow rates ranging from 0.1 to 1 l/min was used as a coolant. The results showed a better thermal performance of the single configuration as it produced an enhancement of 35% in Nusselt number and a reduction in the thermal resistance by 19%. Flowed by the double one then the triple path microchannel, however, the enhancement of the heat transfer was at the expense of the expressively larger pressure drop. The literature survey can conclude that the liquid cooling method is more suitable than air cooling method to dissipate the generated heat by the new generation of GPU and CPU also the heatsink configuration and channel shapes have a significant effect on the heat dissipation process. Therefore, in this work the hydrothermal performance of a new channel configuration (Archimedean spiralchannel configuration) is studied in terms of CPU temperature, thermal resistance, Nusselt number and pressure drop using water as a coolant at wide range of Reynolds number varies from 3000 to 15000.

II. MODELING AND NUMERIC

2.1 Computation domain

The computational domain of this work consists of four (4) components of different materials; CPU, glue layer, Coldplate, and liquid water. The CPU is modeled as a square plate with dimensions of 65mm x 65mm x 3mm and is made of alumina. The CPU sticks to the Coldplate of the heatsink using an ethoxy thin (200 μm) layer. The Coldplate is modeled as a circular disc of 105 mm in diameter and 7.1 mm in thickness. The heatsink is made of copper as it has good machinability and highthermal conductivity. Finally, the liquid water domain is made of a rectangular channel that is grooved into the Coldplate. The material properties of Alumina, ethoxy, copper, and water are listed in Table 2. The Archimedean spiral channel has cross-section dimensions of 3 mm x 5 mm. The channel path is constructed using the Archimedean spiral curve which can be mathematically described by [15]:

$$x = At\cos(\frac{t}{2\pi}) \quad (1)$$

$$y = At\sin(\frac{t}{2\pi}) \quad (2)$$

Where x and y represent a set of points equivalent to the positions of a point moving away from the curve center. The channel width can be controlled by varying the parameter A. while the parameter t is used to extend the channel outer diameter up to 100 mm. The channel's wall thickness is o.5 mm. Detailed channel dimensions are presented in Table 1. The coolant which is water is allowed to enter the configuration at the Cold plate's center to facilitate the heat removal process as the heat intensifies at the center as indicated in Figure 1.

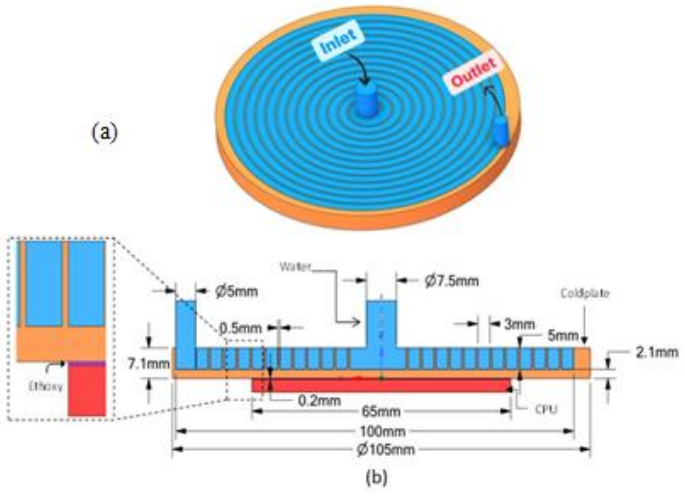

Figure 1: Archimedean Spiral channel heat sink (a) 3D view (b) cross-section view

International Research Journal of Innovations in Engineering and Technology (IRJIET)

ISSN (online): 2581-3048

Volume 6, Issue 8, pp 61-71, August-2022

https://doi.org/10.47001/IRJIET/2022.608009

Table 1: Channel Dimensions

Channel	Single
W_{ch}	3 mm
H_{ch}	5 mm
δ_{wall}	0.5 mm
D_h	3.75 mm
***Archimedean* Curve**	
Start (t)	8.5
End (t)	89.7597901
A	3.5
Y	49.99956058
X	0.209622066
Coldplate	
D	105mm
H	7.1 mm

Table 2: Material properties

Properties	Water	Copper	Ethoxy	Alumina
Density [Kg/m^3]	998.2	8978	2300	3900
Specific Heat [J/(Kg.K)]	4182	381	1460	900
Thermal Conductivity[W/(m.k)]	0.6	387.6	2.2	27
Viscosity [Kg/m.s]	0.001003	-------	-------	-------

2.2 Governing equations (Navier-Stokes Equations)

Navier-Stokes equations describe mathematically the physical relation between the flow variable i.e, velocity, and pressure for incompressible flow, in addition to density for compressible flow. The relation between flow variables is very complicated due to the nonlinearity built in the nature of the Navier Stokes equations, especially the convective term. The flow velocity is a vector of the three components while the pressure has no directional meaning. For affordable computational cell size, the Navier Stokes solver never converges and sometimes crashes for high Reynolds numbers due to instabilities build in the mathematical and physical nature of the Navier Stokes equations[16]. To eliminate the instabilities arising from the instantaneous fluctuation in flow velocity and pressure, time averaging is introduced such that the instantaneous flow variable is split into the average and fluctuation part ($\mathbf{u} = \bar{\mathbf{u}} + \mathbf{u}', \boldsymbol{p} = \bar{\boldsymbol{p}} + \boldsymbol{p}'$). Substitute into the Navier Stokes equations results in what is commonly known as the Reynolds Average Navier Stokes equations (RANS). The RANS has a closure problem that needs to be addressed using turbulence models as will be discussed later [17].The flow conditions in the liquid domain are assumed as single-phase, steady, incompressible, constant density, and non-reacting flow. The Navier Stokes equation can be expressed as:

Continuity:

$$\frac{\partial \bar{u}_i}{\partial x_i} = 0 \qquad (3)$$

Momentum:

$$\frac{\partial \mathrm{u}}{\partial t} + (\mathrm{u}.\nabla)\mathrm{u} = -\nabla p + \frac{1}{Re}\nabla^2 \mathrm{u} \qquad (4)$$

The Reynolds average of the instantaneous momentum equation introduces The Reynolds stress tensor ($R_{ij} = \rho\overrightarrow{u_i u_j}$) which is the closure problem of momentum's equation and it's modeled based on Boussinesq eddy-viscosity approximation such as:

$$R_{ij} = \rho\overrightarrow{u_i' u_j'} = \mu_t\left(\frac{\partial \bar{u}_i}{\partial x_j} + \frac{\partial \bar{u}_j}{\partial x_i}\right) - \frac{2}{3}\rho k\delta_{ij} \qquad (5)$$

The used turbulence model in this work is SST model that introduced In 1994 [18,19] by Menter. This model is a hybrid one, it combines the $k-\varepsilon$ and $k-\omega$ model advantages as it switches to $k-\varepsilon$ away from channel wallsand to$k-\omega$ near wall region, according to:

$$\nu_t = \frac{a_1 k}{\max(a_1\omega, \Omega F_2)} \qquad (6)$$

k and ωcan be estimated by solving the transport equations shown below:

$$\frac{\partial \mathrm{k}}{\partial \mathrm{t}} + \bar{\mathrm{u}}_\mathrm{j}\frac{\partial \mathrm{k}}{\partial \mathrm{x}_\mathrm{j}} = \left(\frac{\partial \bar{\mathrm{u}}_\mathrm{i}}{\partial \mathrm{x}_\mathrm{j}} + \frac{\partial \bar{\mathrm{u}}_\mathrm{j}}{\partial \mathrm{x}_\mathrm{i}}\right)\frac{\partial \bar{\mathrm{u}}_\mathrm{i}}{\partial \mathrm{x}_\mathrm{j}} - \beta'\,\omega\mathrm{k} + \frac{\partial}{\partial \mathrm{x}_\mathrm{j}}\left[(\nu + \sigma_\mathrm{k}\nu_\mathrm{t})\frac{\partial \mathrm{k}}{\partial \mathrm{x}_\mathrm{j}}\right] \qquad (7)$$

$$\frac{\partial \omega}{\partial \mathrm{t}} + \bar{\mathrm{u}}_\mathrm{j}\frac{\partial \omega}{\partial \mathrm{x}_\mathrm{j}} = \frac{\lambda}{\nu_\mathrm{t}}\left(\frac{\partial \bar{\mathrm{u}}_\mathrm{i}}{\partial \mathrm{x}_\mathrm{j}} + \frac{\partial \bar{\mathrm{u}}_\mathrm{j}}{\partial \mathrm{x}_\mathrm{i}}\right)\frac{\partial \bar{\mathrm{u}}_\mathrm{i}}{\partial \mathrm{x}_\mathrm{j}} - \beta\omega^2 + \frac{\partial}{\partial \mathrm{x}_\mathrm{j}}\left[(\nu + \sigma_\omega\nu_\mathrm{t})\frac{\partial \omega}{\partial \mathrm{x}_\mathrm{j}}\right] + 2(1 - \mathrm{F}_1)\frac{\sigma_{\omega 2}}{\omega}\frac{\partial \mathrm{k}}{\partial \mathrm{x}_\mathrm{j}}\frac{\partial \omega}{\partial \mathrm{x}_\mathrm{j}} \qquad (8)$$

The values of model parameters ($\beta', \sigma_k, \lambda, \beta, \sigma_\omega, \sigma_{\omega 2}$) are given in [18,19]. After the convergence of the continuity and momentum equations, the energy equation as a transport equation is solved iteratively, for fluid and solid computational domains can be expressed as [20]

$$\rho\left(u_i\frac{\partial T_f}{\partial x_i}\right) = \mu Pr\left(\frac{\partial^2 T_f}{\partial x_i^2}\right) \qquad (1)$$

$$\left(\frac{\partial^2 T_s}{\partial x_i^2}\right) = 0 \qquad (2)$$

The equations above are solved iteratively to provide a temperature field for solid domains and pressure, velocity as well as temperature for liquid water domain.

International Research Journal of Innovations in Engineering and Technology (IRJIET)

ISSN (online): 2581-3048

Volume 6, Issue 8, pp 61-71, August-2022

https://doi.org/10.47001/IRJIET/2022.608009

2.3 Grid generation

The most important step in computational fluid dynamics is to discretize the domain into tiny computational elements known as cells. That helps to apply thermal and mechanical equilibrium conditions to the system to simplify applying the fundamental physical principles to the computational domainas it's divided into very small systems with constant pressure, Temperature, and other thermophysical proprieties. Hence the thermal equilibrium condition can be assumed with acceptable accuracy.

As the mesh should be fine enough to capture the flow features, a mesh-independent study should be done to get a grid-independent solution as it's basically to use a coarse mesh size and then refine it gradually while monitoring an output parameter such as the coolant outlet temperature that's sensitive enough to mesh size[17]. When the output parameter no longer varies with the number of cells (approaches a steady condition) it can be assumed that the physics variations could be captured by the corresponding mesh size. Figure 2 indicates that the coolant's outlet temperature shows no significant variation beyond two million cells. However, further refinement up to 5.8 million was needed for the fluid domain to capture the velocity profile in the Archimedean spiral channel.

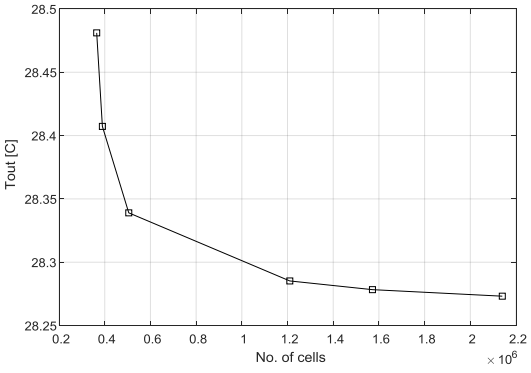

Figure 2: Mesh independent study

2.4 Boundary conditions

The boundary conditions used to simulate the computational domain are:

- Fluid: The boundary conditions of the fluid domain at the inlet are the velocity in (m/s) which is a function of Re as it changes from 3000 to 15000 ($\boldsymbol{V_{in}}$=$\boldsymbol{f}$(Re)) and Temperature which is kept unchanged ($\boldsymbol{T_{in}}$ =25°C). Where the outlet pressure is assumed atmospheric (P=0 atm). The upper surface, the entrance, and the existence of the fluid are considered adiabatic.
- Solid: all the external walls of the solid domains are considered adiabatic ($\boldsymbol{q^{\bullet}=0}$) except for the CPU bottom surface which is subjected to a constant heat flux based on the dissipated power of 450 W (q=$\frac{\boldsymbol{Q}}{\boldsymbol{A}}$= 106,508.875 W/$\boldsymbol{m^2}$).
- Interface: several interfaces are existed such as the fluid-Coldplate, Coldplate-Ethoxy, and Ethoxy-CPU interface as the temperature on each one of them is $T_{fuid} = T_{Coldplate}$, $T_{Coldplate} = T_{Ethoxy}$, and $T_{Ethoxy} = T_{CPU}$ respectively.

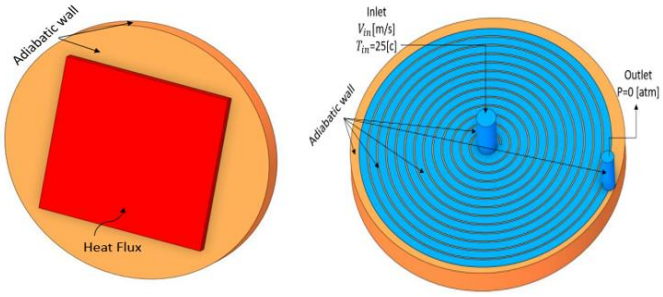

Figure 3: The 3D Archimedean spiral channel with boundary conditions

2.5 Data Reduction

The hydrothermal performance of the Archimedean spiral channel can be obtained using the Performance Evaluation criterion equation (PEC) which depends on two factors: (1) the fanning friction factor (f) determines the required pumping power and (2) the Nusselt number (Nu) which expresses the channel's performance in heat transfer rate, as shown below [10,21]

$$\mathrm{PEC} = \frac{(\mathrm{Nu}/\mathrm{Nu}_0)}{(\mathrm{f}/\mathrm{f}_0)^{1/3}} \qquad (11)$$

Where $f_0$and Nu_0representthe fanning friction factor and the Nusselt Number of the straight channel using the Blasius equation for the fanning friction factor [$f_0 = 0.079\mathrm{Re}^{-0.25}$][22,23] and (Dittus and Boelter) equation for Nusselt number ($Nu_0 = 0.023\mathrm{Re}^{0.8}\mathrm{Pr}^{0.4}$)[24]. The f and Nu represent the fanning friction factor and the Nusselt Numberof the Archimedean spiral channel configuration respectively [25].

$$\mathrm{Nu} = \frac{\mathrm{h_m D_h}}{\mathrm{k_f}} = \frac{\dot{m}\mathrm{c_p}\ (\mathrm{T_{out}} - \mathrm{T_{in}})}{\mathrm{A_s}\ (\mathrm{T_s} - \frac{\mathrm{T_{out}} + \mathrm{T_{in}}}{2})} \frac{\mathrm{D_h}}{\mathrm{k_f}} \qquad (12)$$

Where D_h is the channel's hydraulic diameter, k_f is the fluid's conductivity and $h_m$is the average heat transfer coefficient which is calculated by:

International Research Journal of Innovations in Engineering and Technology (IRJIET)

ISSN (online): 2581-3048

Volume 6, Issue 8, pp 61-71, August-2022

https://doi.org/10.47001/IRJIET/2022.608009

$$h_m = \frac{qA_{CPU}}{A_s(T_s - T_m)} \qquad (13)$$

q represents the heat flux subjected to the bottom of the CPU,A_{cpu} the surface area of the CPU, A_s and T_s are the area and the temperature of the interface between the fluid and the cold plate, and T_m is the mean fluid temperature and can be simplified using:

$$T_m = \frac{T_{in} + T_{out}}{2} \qquad (14)$$

The fanning friction factor can be calculated from the equation indicated below[22]:

$$f = \frac{\Delta P D_h}{2 * \rho_f u_{in}^2 L} \qquad (15)$$

Here, ΔP is the pressure drop across the channel length L, u_{in} is the inlet velocity and ρ_f is the density of the coolant.

To measure the resistance of the materials used for all domains (CPU, Thermal paste, Coldplate, and coolant) to dissipate the input power, the thermal resistance (R) should be introduced [26,27]:

$$R = \frac{T_{max} - T_f}{q} \text{ (K/W)}$$

Where q is the heat flux imposed on the CPU, T_{max} is the temperature of the bottom surface of the CPU and T_f is the inlet water temperature.

III. RESULTS AND DISCUSSIONS

3.1 Validation

To validate the computational scheme used in this work, a comparison is conducted with experimental data reported by Jilte et al.[12]. The experiment was conducted on a heat sink model shown in ***Figure 1***, which has a different configuration than the current work model. The CFD settings are kept unchanged while the heat sink is remodeled to be aligned with the experimental model. The experimental model consisted of four channels of 3.5 mm in depth and 4 mm in width. Liquid water was used as a coolant and several openings were made in the channel walls spaced by 180° to allow the water to move from one pass to another. The heat flux applied to the bottom surface was based on the dissipated power of 50 W and 70W.The outlet fluid temperature was selected for comparison at different flow rates of 60 to 180 ml/min. The highest deviation recorded is about 5% at lower flow rates namely 60-100 ml/min. However, it can be seen from ***Figure 5*** that the numerical results agree with the previous study, especially for higher flow rates (>120 ml/min). This can conclude that CFD settings can be used, with acceptable confidence, as a tool to analyze the conjugate heat transfer in the heat sink.

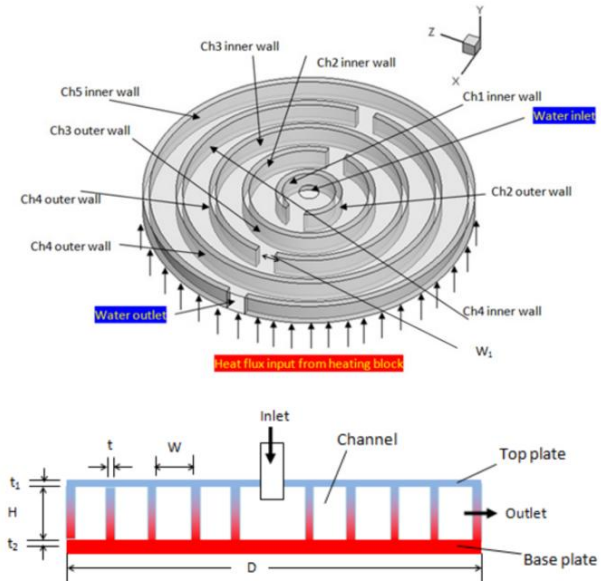

Figure 4: Circular heat sink used for validation[12]

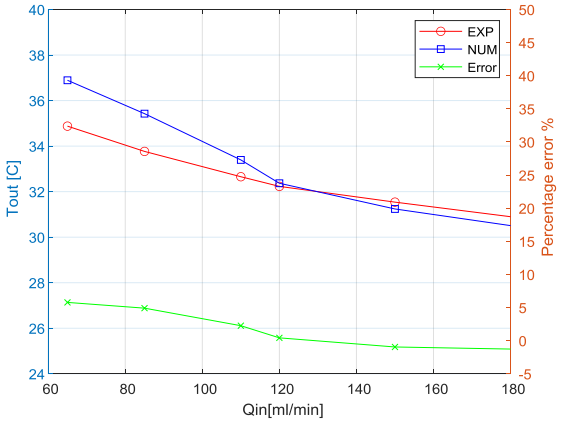

Figure 5: Results of the validation

3.2 Temperature field

The temperature contour of the cross-sectional view of all domains in **Figure 7** indicates that the maximum Temperature resides in the CPU as a result of imposing the heat flux on the bottom surface of it, the temperature of the cooling liquid is getting higher as it moves along the channel toward the outlet until it gets the same temperature as the channel walls, because of the heat transfer that takes place between the coolant and the Coldplate, and with increasing the Reynolds number the difference in temperature between the inlet and outlet of the coolant decreases. It could be also noted from the results shown in ***Figure 6***that the maximum and average temperatures of CPU show a nonlinear rapid drop with Re. the CPU temperature changes dramatically for Reynolds number

International Research Journal of Innovations in Engineering and Technology (IRJIET)

ISSN (online): 2581-3048

Volume 6, Issue 8, pp 61-71, August-2022

https://doi.org/10.47001/IRJIET/2022.608009

(3000-8000) while the rate of change decreases for Reynolds number (8000-15000). The average temperature developed within the CPU decreases with Re according to $T_{avg} = 45.96 + \frac{4793}{\mathrm{Re}^{0.886}}$ in °C. The temperature across the Archimedean spiral channel is heterogeneously distributed as the non-symmetrical temperature profile as the water with higher temperature remains on the outer side of the channel wall, because of the non-symmetrical velocity profile. See **Figure *11***.

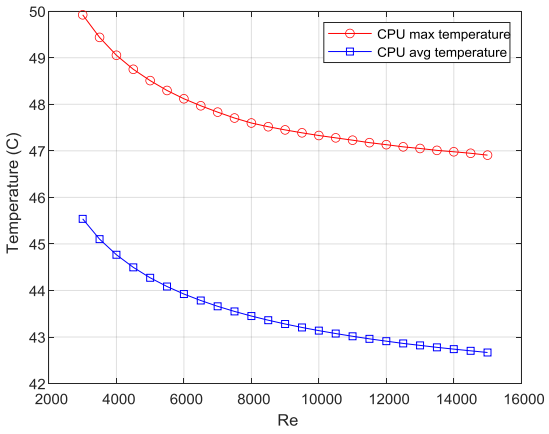

Figure 6: The variation of CPU temperature with Re

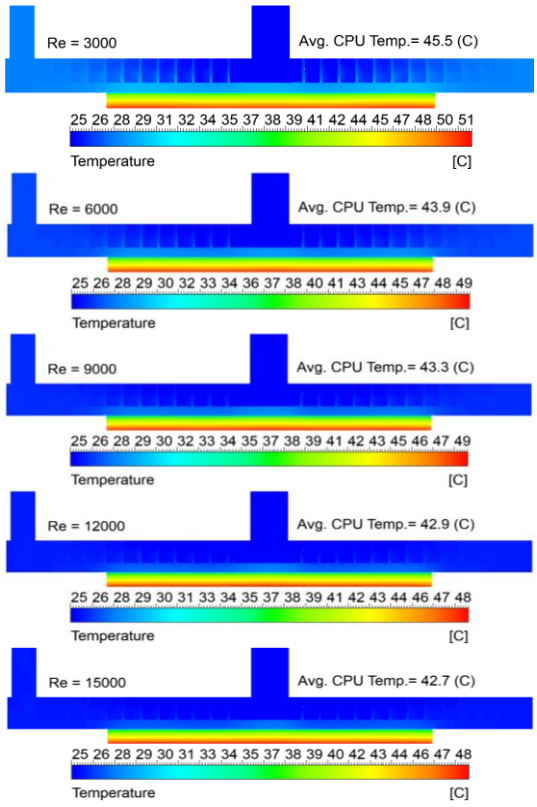

Figure 7: Temperature contour of all computational domains

3.3 Pressure field

The pressure drop for laminar flow is independent of the roughness of the surface, it increases with the fluid viscosity and the equivalent channel length and decreases with the squared channel hydraulic diameter. While in turbulent flow the pressure drop gets affected by the surface roughness along with the fluid density, average velocity, and the length and hydraulic diameter of the channel. The pressure drop is essential to estimate the required pumping power to get the heat sink's hydrothermal performance. **Figure 8** indicates that the Archimedean spiral channel develops a maximum pressure drop at Re =15000 of about 1000 kPa and a minimum pressure drop of about 75 kPa at Re = 3000. It increases at an exponential rate with Re according to $\Delta P = 0.05494\mathrm{Re}^{1.755}$ in Pa.

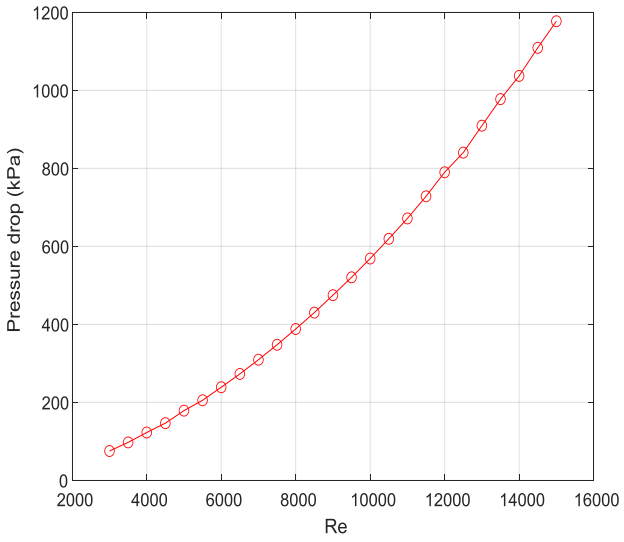

Figure 8: The pressure drop across the Archimedean spiral channel

Darcy-Weisbach equation confirms these findings for internal flow when the pressure drop depends on the squared average velocity. The pressure of fluid can be observed to be higher in the center of the cold plate then it drops along the channel to the outlet, as indicated by the contours of the pressure drop computed in **Figure 9** that occur in the Archimedean spiral channel configuration at the plane located at the middle of the channel depth.

International Research Journal of Innovations in Engineering and Technology (IRJIET)

ISSN (online): 2581-3048

Volume 6, Issue 8, pp 61-71, August-2022

https://doi.org/10.47001/IRJIET/2022.608009

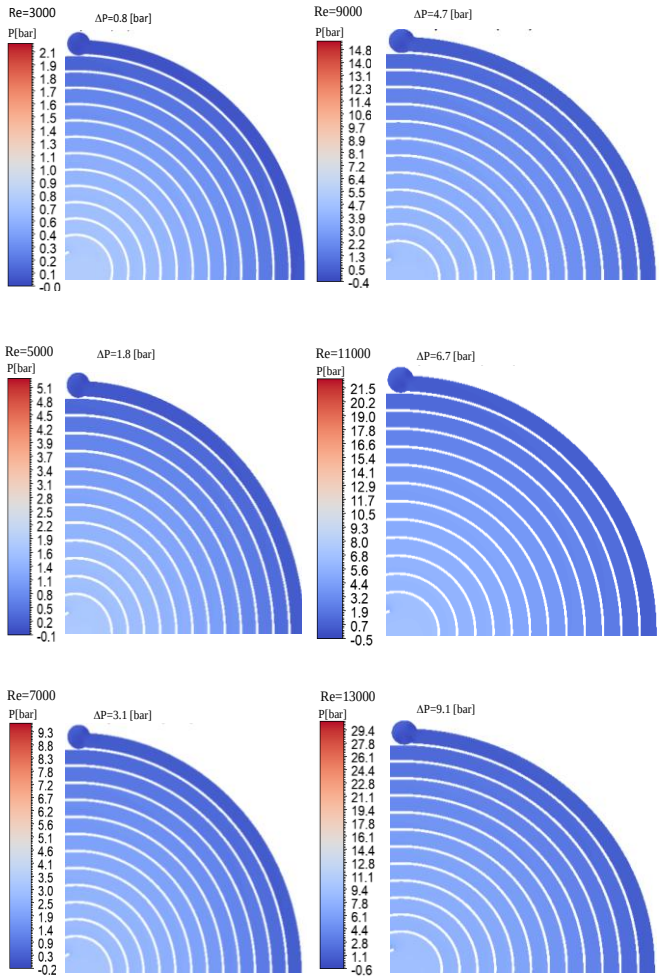

Figure 9: Pressure drop contours

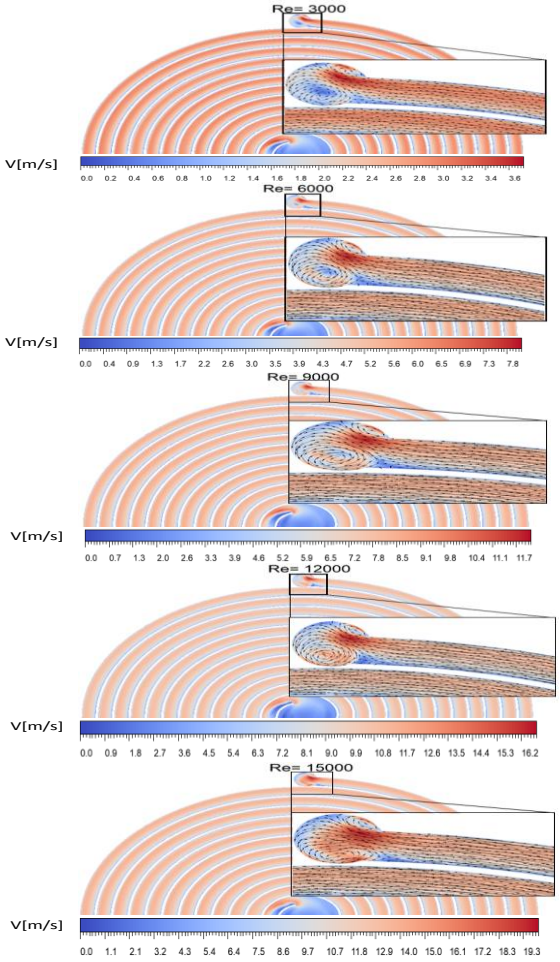

Figure 10: Velocity contours in the Archimedean spiral channel

3.4 Flow structure

The flow structure of the coolant in the Archimedean spiral channel is indicated by the velocity contours in Figure 10 that occur in the Archimedean spiral channel configuration at the plane located in the middle of the channel depth. The fluid's average velocity in the spiral channel changes from zero at the channel walls due to the no-slip condition, to the maximum value near the inner channel wall away from the center of the channel because of the effect of the additional centrifugal force in the Archimedean spiral channel on the velocity profile as shown in Figure 11.

The entrance configuration causes secondary flow which is vorticity in the flow field because of the gradient in the velocity as shown in Figure 12. It was also noticed at the exit portion; the vortices intensify with higher Reynolds numbers. This phenomenon is expected to have a good influence on the enhancement of the heat transfer however, it intensifies the pressure drop.

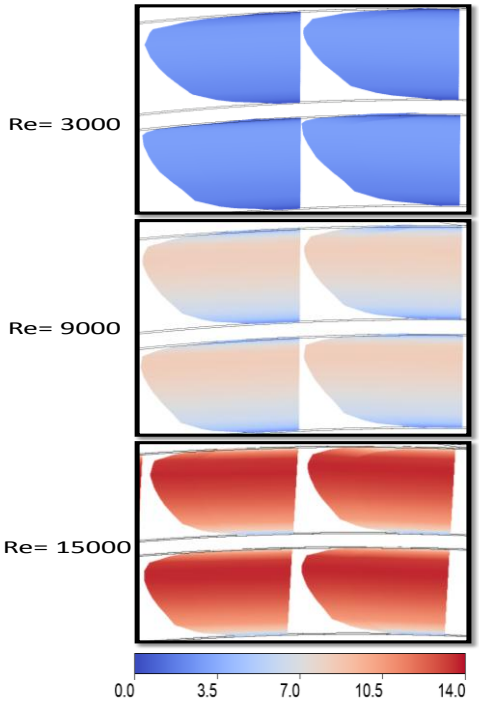

Figure 11: Velocity profile in Archimedean spiral channel

International Research Journal of Innovations in Engineering and Technology (IRJIET)

ISSN (online): 2581-3048

Volume 6, Issue 8, pp 61-71, August-2022

https://doi.org/10.47001/IRJIET/2022.608009

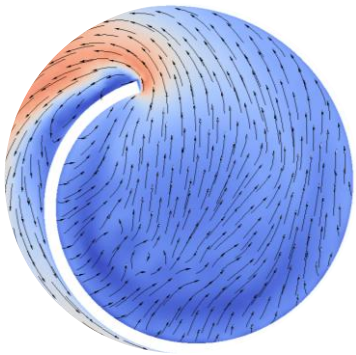

Figure 12: The entrance of the Archimedean spiral channel configuration

3.5 Nusselt Number

The variation of the average Nusselt number for Archimedean spiral channel with Reynolds number is indicated in Figure 13. It shows that the Nu increases with increasing the Re. The Archimedean spiral channel develops significant enhancement in Nu compared to the straight channel, this enhancement increases with increasing Re. As the results showed that the Archimedean spiral channel's Nu increases 54% at Re= 15000 and 50% at Re=3000 relative to the straight channel. Nu correlates with Re according to $Nu=0.0328\ Re^{0.85}\ Pr^{0.4}$with a coefficient of determination of 0.9999. This is compared with the Dittus-Boelter correlation that is used for straight channel ($Nu=0.023\ Re^{0.8}\ Pr^{0.4}$). The Prandtl number (Pr) is determined at the average temperature of the water.

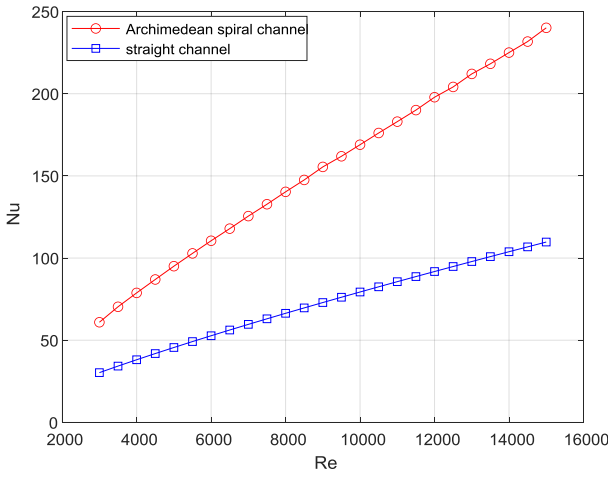

Figure 13: The variation of Nusselt number with Re

3.6 Thermal Resistance

The thermal resistance has complete control over the temperature variation across computational domains. For instance, the copper plate which has lower thermal resistance (higher thermal conductivity) shows less gradient in temperature compared with the CPU made of alumina which has lower thermal conductivity, as shown in Figure 14. The total thermal resistance of the Archimedean spiral channel as a function of Re for an inlet coolant temperature of 25°C and input power of 450 W is shown in Figure 15. As it's clear that the R decreases with increasing Re. This can be projected on the drop of CPU temperature with increasing Re.

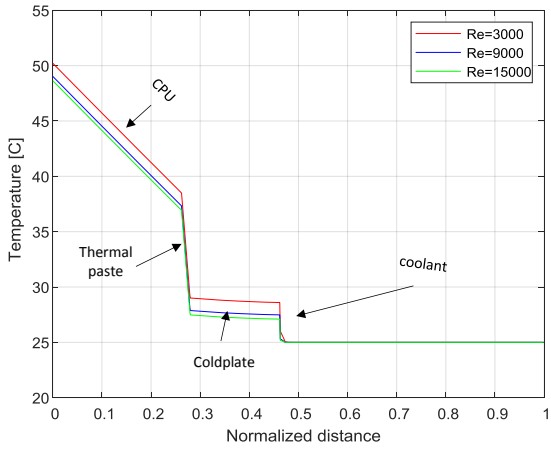

Figure 14: The temperature gradient across each computational domain

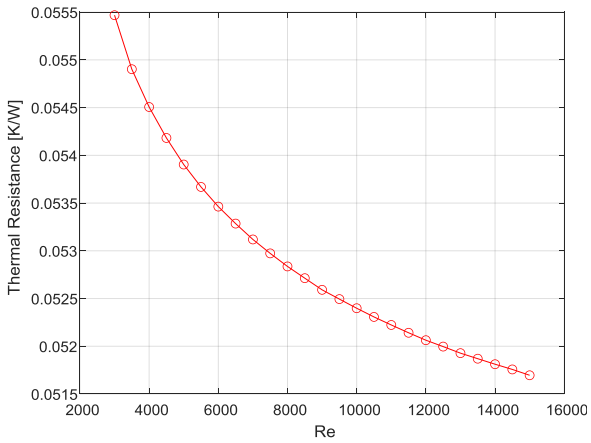

Figure 15: The variation of the total thermal resistance with Re

3.7 Turbulence

Turbulence plays a critical role in the transport of heat and mixing. Figure 16 shows the distribution of the turbulent kinetic energy which is defined as energy taken from mean flow to feed the turbulent eddies[16]. The SST turbulent model is essentially based on the Boussinesq approximation in which the Reynolds stress tensor is assumed to be correlated with the velocity gradient tensor. Not to forget that this assumption is still controversial among the turbulence community. This is because the Boussinesq hypothesis is used originally to link the shear stress with velocity gradient using molecular viscosity. However, in turbulence, the eddy viscosity is a kinematic rather than molecular property. Nevertheless, the eddy viscosity seems to work well for channel mean flow. Since the velocity gradient tensor is the

International Research Journal of Innovations in Engineering and Technology (IRJIET)

ISSN (online): 2581-3048

Volume 6, Issue 8, pp 61-71, August-2022

https://doi.org/10.47001/IRJIET/2022.608009

driving force for Reynolds stress, therefore, regions with higher velocity gradient are developing higher turbulent kinetic energy as shown in Figure 16. Once again, the Archimedean channel broke the symmetry where the turbulent kinetic energy is generated at higher rate next to the outer channels' wall compared with the inner wall. This is supported by the velocity profile depicted in Figure 11 where the higher velocity gradient is developed in the boundary layer of the outer wall.

3.8 Hydrothermal Performance

The hydrothermal performance of the Archimedean spiral channel with Re is shown in *Figure 17* according to the PEC equation, it's obvious that the hydrothermal performance is higher at lower Re as it drops exponentially with increasing Re. At high Re (8000-15000), the rate at which PEC drops is much lower for Re (3000-6000). This is a shred of important evidence for approaching a specific flow condition and channel configuration under a specific limitation of CPU temperature. The PEC's exponential drop can be projected on the pressure drop at high Reynolds numbers. We can conclude that better hydrothermal performance could be obtained at lower flow velocities.

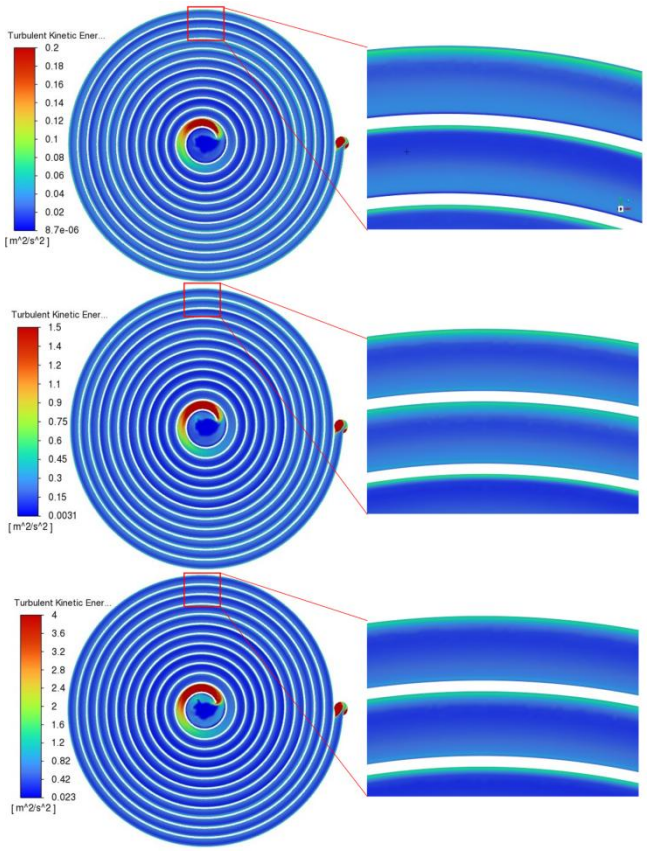

Figure 16: Turbulent kinetic energy contours at different Re

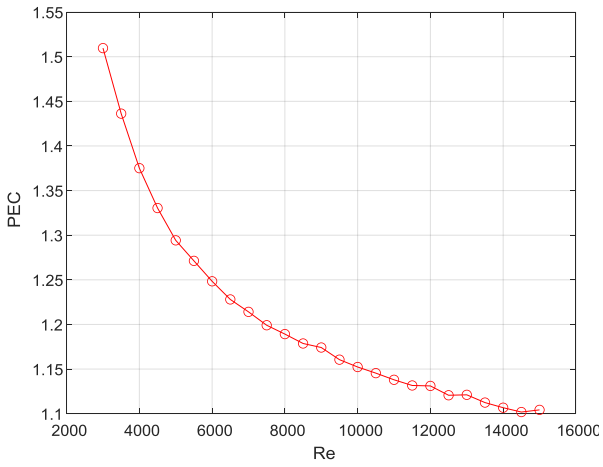

Figure 17: The variation of the Performance Evaluation criterion in the Archimedean spiral channel with Re

IV. CONCLUSION

In this work the hydrothermal characteristics in the Archimedean spiral channel configuration are numerically studied, the heatsink model consists of an Archimedean spiral channel grooved into a circular copper plate of 105 mm diameter, attached to a rectangular (65mm x 65mm) alumina CPU by an 0.2 mm ethoxy thermal paste layer, water is used as a coolant at an inlet temperature of 25°C and a range of inlet velocity as a function of Re varies from 3000 to 15000.Input power of 450 W was subjected to the bottom surface of the CPU, all other external walls of the solid domains are considered adiabatic. The Shear Stress Transport (k-ω SST) is the used turbulent model for a better capturing of the viscous, high-frequency flow fluctuation near-wall region, the conclusions that can be drawn from this work are:

1. The overall cooling performance of the Archimedean spiral channel is good as it reduces the CPU average temperature for the whole Re used range below 46 °C.
2. The Re has a decisive impact on the cooling performance, as the temperature of CPU changes with Re according to $T_{avg} = 45.96 + \frac{4793}{Re^{0.886}}$.
3. The Archanmidean spiral channel develops significant enhancement in Nu compared to the straight channel, this enhancement increases with increasing Re. the Archimedean spiral channel's Nu increases 54% at Re= 15000 and 50% at Re=3000 relative to the straight channel. Nu correlates with Re according to $Nu=0.0328\ Re^{0.85}\ Pr^{0.4}$ with a coefficient of determination of 0.9999.
4. The Archimedean spiral channel shows a better hydrothermal performance at lower Re as it drops exponentially with increasing Re, At high Re (8000-15000), the rate at which PEC drops is much lower for Re (3000-6000).
5. The Archimedean spiral channel broke the symmetrical structure of the turbulent kinetic energy. Induced by a

ISSN (online): 2581-3048
Volume 6, Issue 8, pp 61-71, August-2022
https://doi.org/10.47001/IRJIET/2022.608009

higher velocity gradient, the region next to the outer channels' wall develops a higher rate of turbulent kinetic energy.

REFERENCES

[1] Yang D, Yao Q, Jia M, Wang J, Zhang L, Xu Y, et al. Application analysis of efficient heat dissipation of electronic equipment based on flexible nanocomposites. Energy and Built Environment 2021;2:157–66. https://doi.org/10.1016/j.enbenv.2020.07.008.

[2] Deng Y, Liu J. Design of practical liquid metal cooling device for heat dissipation of high performance CPUs. Journal of Electronic Packaging, Transactions of the ASME 2010;132:1–6. https://doi.org/10.1115/1.4002012.

[3] Chan A, Wei J. Study on Alternative Cooling Methods Beyond Next Generation Microprocessors. vol. 2. 2003. https://doi.org/10.1115/IPACK2003-35041.

[4] Nada SA, El-Zoheiry RM, Elsharnoby M, Osman OS. Experimental investigation of hydrothermal characteristics of data center servers' liquid cooling system for different flow configurations and geometric conditions. Case Studies in Thermal Engineering 2021;27. https://doi.org/10.1016/j.csite.2021.101276.

[5] L.Boylestad R, Nashelsky L. electronic devices and circuit. 2014.

[6] Bahiraei M, Heshmatian S. Efficacy of a novel liquid block working with a nanofluid containing graphene nanoplatelets decorated with silver nanoparticles compared with conventional CPU coolers. Applied Thermal Engineering 2017;127:1233–45. https://doi.org/https://doi.org/10.1016/j.applthermaleng.2017.08.136.

[7] Bahiraei M, Heshmatian S, Goodarzi M, Moayedi H. CFD analysis of employing a novel ecofriendly nanofluid in a miniature pin fin heat sink for cooling of electronic components: Effect of different configurations. Advanced Powder Technology 2019;30:2503–16. https://doi.org/10.1016/j.apt.2019.07.029.

[8] Zhang HY, Pinjala D, Teo PS. Thermal management of high power dissipation electronic packages: From air cooling to liquid cooling. Proceedings of 5th Electronics Packaging Technology Conference, EPTC 2003 2003:620–5. https://doi.org/10.1109/EPTC.2003.1271593.

[9] Tuckerman DB, Pease RFW. High-Performance Heat Sinking for VLSI. IEEE Electron Device Letters 1981;EDL-2:126–9. https://doi.org/10.1109/EDL.1981.25367.

[10] Khan MZU, Younis MY, Akram N, Akbar B, Rajput UA, Bhutta RA, et al. Investigation of heat transfer in wavy and dual wavy micro-channel heat sink using alumina nanoparticles. Case Studies in Thermal Engineering 2021;28. https://doi.org/10.1016/j.csite.2021.101515.

[11] Fan, Yanfeng and Hassan I. Investigation of cooling performance of a swirl microchannel heat sink by numerical simulation. International Conference on Nanochannels, Microchannels, and Minichannels, 2011, p. 463--469.

[12] Jilte R, Ahmadi MH, Kumar R, Kalamkar V, Mosavi A. Cooling performance of a novel circulatory flow concentric multi-channel heat sink with nanofluids. Nanomaterials 2020;10. https://doi.org/10.3390/nano10040647.

[13] Al-neama AF, Khatir Z, Kapur N, Summers J, Thompson HM. International Journal of Heat and Mass Transfer An experimental and numerical investigation of chevron fin structures in serpentine minichannel heat sinks. International Journal of Heat and Mass Transfer 2018;120:1213–28. https://doi.org/10.1016/j.ijheatmasstransfer.2017.12.092.

[14] Al-Neama AFM. Serpentine minichannel liquid-cooled heat sinks for electronics cooling applications 2018.

[15] Umehara M, Yamada K, Rossman W. Differential Geometry Of Curves And Surfaces. World Scientific Publishing Company; 2017.

[16] Pope SB, Eccles PJ, Pope SB, Press CU. Turbulent Flows. Cambridge University Press; 2000.

[17] Ozturk E. CFD ANALYSES OF HEAT SINKS FOR CPU COOLING WITH FLUENT. CWL Publishing Enterprises, Inc, Madison 2004;2004:352.

[18] Menter FR, Kuntz M, Langtry R. Ten Years of Industrial Experience with the SST Turbulence Model 2003.

[19] Rocha PAC, Rocha HHB, Carneiro FOM, Vieira da Silva ME, Bueno AV. K-ω SST (shear stress transport) turbulence model calibration: A case study on a small scale horizontal axis wind turbine. Energy 2014;65:412–8. https://doi.org/10.1016/j.energy.2013.11.050.

[20] Mokrane M, Lounis M, Announ M, Ouali M, Djebiret MA, Bourouis M. Performance Analysis Of A Micro Heat Exchanger In Electronic Cooling Applications. Journal of Thermal Engineering 2021;7:774–90. https://doi.org/10.18186/thermal.929458.

[21] Fan JF, Ding WK, Zhang JF, He YL, Tao WQ. A performance evaluation plot of enhanced heat transfer techniques oriented for energy-saving. International Journal of Heat and Mass Transfer 2009;52:33–44.

ISSN (online): 2581-3048
Volume 6, Issue 8, pp 61-71, August-2022
https://doi.org/10.47001/IRJIET/2022.608009

https://doi.org/10.1016/j.ijheatmasstransfer.2008.07.006.

[22] Liu J, Hussain S, Wang J, Wang L, Xie G, Sundén B. Heat transfer enhancement and turbulent flow in a high aspect ratio channel (4:1) with ribs of various truncation types and arrangements. International Journal of Thermal Sciences 2018;123:99–116. https://doi.org/10.1016/j.ijthermalsci.2017.09.013.

[23] Mirmanto. Developing Flow Pressure Drop and Friction Factor of Water in Copper Microchannels. Journal of Mechanics Engineering and Automation 2013;3:641–9.

[24] Dittus FW, Boelter LMK. Heat transfer in automobile radiators of the tubular type. International Communications in Heat and Mass Transfer 1985;12:3–22. https://doi.org/10.1016/0735-1933(85)90003-X.

[25] Das L, Rubbi F, Habib K, Saidur R, Islam N, Saha BB, et al. Hydrothermal performance improvement of an inserted double pipe heat exchanger with Ionanofluid. Case Studies in Thermal Engineering 2021;28:101533. https://doi.org/10.1016/j.csite.2021.101533.

[26] Al-Neama AF, Kapur N, Summers J, Thompson HM. An experimental and numerical investigation of the use of liquid flow in serpentine microchannels for microelectronics cooling. Applied Thermal Engineering 2017; 116:709–23. https://doi.org/10.1016/j.applthermaleng.2017.02.001.

[27] Steinke ME, Kandlikar SG. Single-Phase Liquid Heat Transfer in Plain and Enhanced Microchannels. vol. ASME 4th I, 2006, p. 943–51. https://doi.org/10.1115/ICNMM2006-96227.

Citation of this Article:

Hala M. Rashad, Younis M. Najim, Hatem Hasan Ismaeel, "Hydrothermal Analysis of Archimedean Spiral Channel Heat Sink for CPU Cooling", Published in *International Research Journal of Innovations in Engineering and Technology - IRJIET*, Volume 6, Issue 8, pp 61-71, August 2022. Article DOI https://doi.org/10.47001/IRJIET/2022.608009

****

